Using Agents and Unsupervised Learning for Counting Objects in Images with Spatial Organization

Eliott Jacopin[a], Naomie Berda, Léa Courteille, William Grison, Lucas Mathieu, Antoine Cornuéjols[b] and Christine Martin[c]

UMR MIA-Paris, AgroParisTech, INRA, Université Paris-Saclay, 75005, Paris, France

Keywords: Image Processing, Computer Vision, Counting Objects, Multi-Agent Systems, Unsupervised Learning.

Abstract: This paper addresses the problem of counting objects from aerial images. Classical approaches either consider the task as a regression problem or view it as a recognition problem of the objects in a sliding window over the images, with, in each case, the need of a lot of labeled images and careful adjustments of the parameters of the learning algorithm. Instead of using a supervised learning approach, the proposed method uses unsupervised learning and an agent-based technique which relies on prior detection of the relationships among objects. The method is demonstrated on the problem of counting plants where it achieves state of the art performance when the objects are well separated and tops the best known performances when the objects overlap. The description of the method underlines its generic nature as it could also be used to count objects organized in a geometric pattern, such as spectators in a performance hall.

1 INTRODUCTION

Object counting is an important task in computer vision motivated by a wide variety of applications such as crowd counting, traffic monitoring, ecological surveys, inventorying products in stores and cell counting. In agriculture, for instance, Unmanned aerial vehicles (UAVs) allow for cheaper image recording, enabling flexible and immediate image processing (Gnädinger and Schmidhalter, 2017). One critical challenge lies in the automatic counting of plants in fields, if possible at various stages of development.

However, counting objects is difficult as objects are often variable in terms of shape, size, pose and appearance and may be partially occluded. In agriculture, the presence of weeds and blurry effects as well as varying growth stages affect performance.

Existing methods can be categorized mainly into two classes: detection-based and regression-based (Zou et al., 2019).

In the *detection-based* approach, a classifier is learned to recognize the presence of the object(s) of interest in a sub-image or window, and then this window is scrolled through the image in order to count the number of recognized objects. There are however difficulties associated with this approach. First, it requires (very) numerous labeled training examples, often in the form of manually drawn bounding boxes or pixel annotations, which are notoriously costly to acquire. Second, classification of objects is itself a challenging task because of the variability of their appearance, the presence of noise and possible partial occlusions. Besides the selection of relevant descriptors, such as wavelets, shapeless, edgeless, and so on, it requires also the fine-tuning of the parameters of the algorithm. Finally, the choice of the size of a sliding window and of the scrolling process can be tricky.

In contrast, *regression-based* methods attempt to directly estimate the number of objects of interest from an overall characterization of the image. This overcomes most of the difficulties of detection-based methods and, in recent years, these methods have defined the state-of-the-art performances, specially through the use of convolutional neural networks. However, lots of training images as well as advanced expertise to train deep neural networks are still required. In addition, retraining is needed when the objects of interest change.

In this paper, we introduce a novel approach, valid when the objects of interest have regular spatial relationships, like spectators in a performance hall, goods on the shelves of a retail store or plants in fields. It

[a] https://orcid.org/0000-0002-4568-283X
[b] https://orcid.org/0000-0002-2979-3521
[c] https://orcid.org/0000-0003-3956-4789

Jacopin, E., Berda, N., Courteille, L., Grison, W., Mathieu, L., Cornuéjols, A. and Martin, C.
Using Agents and Unsupervised Learning for Counting Objects in Images with Spatial Organization.
DOI: 10.5220/0010228706880697
In *Proceedings of the 13th International Conference on Agents and Artificial Intelligence (ICAART 2021) - Volume 2*, pages 688-697
ISBN: 978-989-758-484-8

works in two phases. First, the approximate spatial relationships between objects are estimated. Second, based on the structure thus found, a multi-agent based approach is used where the structure determines the initial positions of the agents as well as a hierarchy of control agents and therefore a set of communication channels between the agents. Each agent is a weak classifier which guesses if it is positioned over an object of interest in the image and can confirm or deny its guess through exchanges with other agents. The second phase is iterative until the agents are no longer undergoing any changes. The number of final agents gives the number of detected objects.

The advantages of the approach are that:

1. it does not require numerous training images since the determination of the structure is unsupervised and the agents themselves are simple detectors.
2. it easily adapts to various conditions on the structure, nature of the objects, their size and appearance
3. it achieves high performances over the variety of experimental conditions tested.

These good properties come from the assumption that a regular structure exists among objects. The approach should therefore not work on crowd counting, or on cells counting for instance. But when a regular structure exists, this knowledge brings a power that should not be wasted.

Figure 1 provides an example of an aerial image of a sunflower field. One can see rows of plants, here in a rather late stage with overlap between plants, shadows of various sizes and patches of weeds, especially on the left side of the image.

Figure 1: Example of an aerial image from a sunflower field.

The paper is structured as follows. Section 2 presents the proposed approach. Information about the generation of synthetic datasets used in the experiments is provided in Section 3 and the results of the experiments are reported in Section 4. Section 5 concludes and gives perspectives on future works.

2 THE METHOD

2.1 Analyzing the Spatial Relationships

Crop fields usually exhibit a geometrical design. The rows of a crop field are indeed usually parallel to each other and evenly spaced. In addition, crops are planted on the basis of a target density which induces an even distance between two consecutive plants.

One main theme of this paper is to underline the interest of researching and exploiting information on the geometry of the objects in the images to be analyzed. For crop fields images, in order to estimate the inter-rows and inter-plants distances, the method presented begins with (i) isolating the green areas of the images; then (ii) rotating the images enough for the rows to be collinear with the Y axis; and, finally, (iii) applies a Fourier Transform (FT) analysis on the signal produced by projecting the coordinates of the green pixels on the X and Y axis.

2.1.1 Image Segmentation

Before estimating the inter-rows and inter-plants distances, it is necessary to identify the areas of the images corresponding to plants. To that end, we used the vegetation index *Excess Green* (*ExG*) in association with Otsu's automatic segmenting method (Otsu, 1979; Guerrero et al., 2012; Guijarro et al., 2011; Pérez-Ortiz et al., 2016). At the end of the segmentation process, the RGB crop fields images are transformed into black and white images, referred as *Otsu images*, where the white pixels are expected to correspond to a plant (crop or weed).

2.1.2 Vertically Adjusting the Images

To ease the estimation of the inter-rows and inter-plants distances, the rotation of all the images of the datasets was computed in order for the crop rows to be oriented along the Y axis. This method succeeds as long as two consecutive rows do not overlap with each other or weed do not cover all the inter-rows space. Should this happen, one can apply a filter to the Otsu images in order to only keep the skeleton of the crop rows in white. This can be implemented with, for example, the midpoint encoding suggested in (Han et al., 2004).

2.1.3 Estimating the Inter-rows and Inter-Plants Distances

Items **1** and **3** on Fig. 2 illustrate how a periodic signals is detected out of a vertically adjusted Otsu

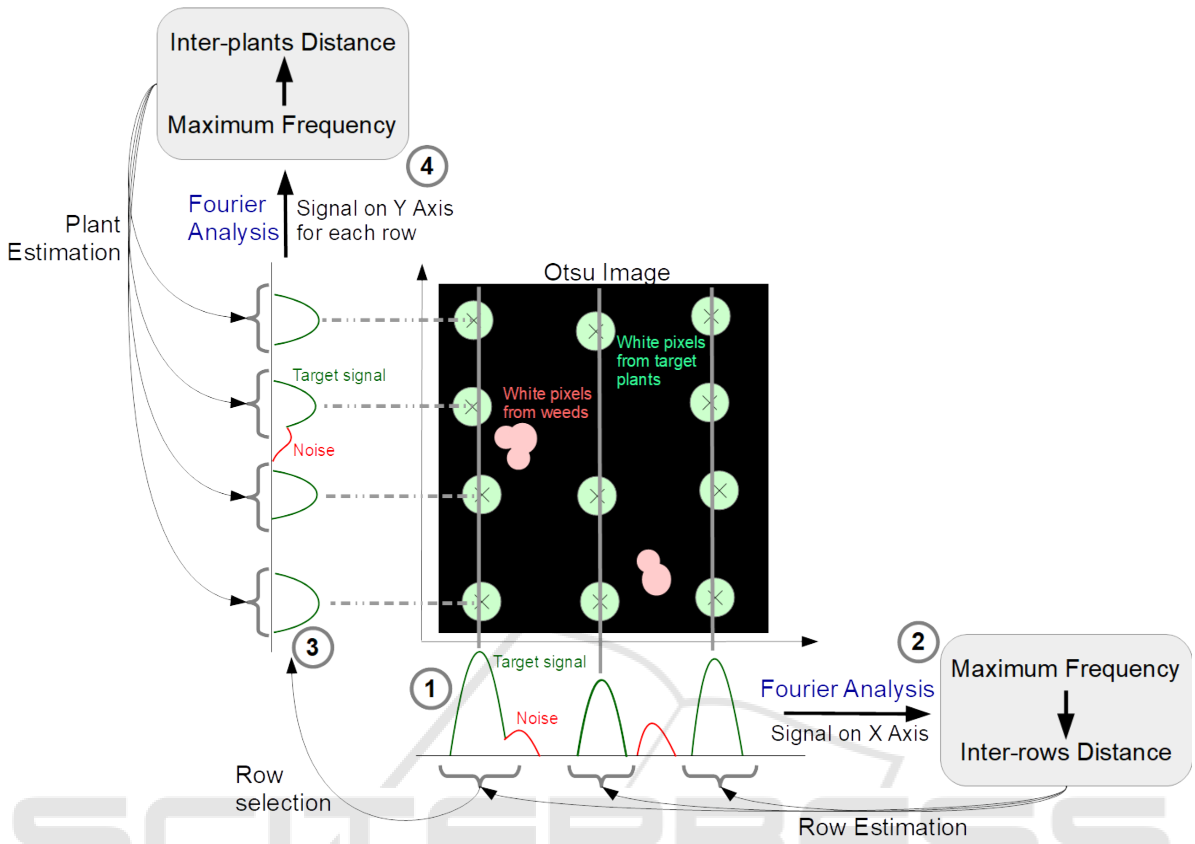

Figure 2: Fourier Analysis on the X and Y axis. The signal processed by the Fourier Transform is made from the projection of the white pixels of the Otsu images on the X and Y axis.

image. Since the rows are assumed to have been re-aligned with the Y axis, the periodicity of the positions of the rows appears on the X axis: the peaks of the density distribution of the white pixels on the X axis mirror the positions of the rows on the image (item **1**). The inter-rows distance is computed using a Fourier analysis on the density distribution and keeping the maximal frequency thus found. The inter-plants distance is then estimated using the projections on the Y axis of the white pixels attributed to each row (items **3** and **4**).

2.2 A Multi-Agent Approach

Just like (Hofmann., 2019) in the case of remote image sensing, we advocate the use of a multi-agent system (MAS) which takes advantage of the knowledge gathered on the geometry in the image. In the context of the plant counting task, we identified four types of agents that are organized hierarchically as shown in Fig. 3. The agent at the top of the system is called the *Director Agent* (DA), then come the *Row Agents* (RAs), the *Plant Agents* (PAs) and finally the *Pixel Agents* (PXAs). Each agent of one layer either acts on its own or receive orders from an agent of the upper layer: there is no communication between agents of the same layer. The environments in which the agents act are the vertically adjusted Otsu images.

2.2.1 The Director Agent

The DA can initialize or destroy RAs according to the predictions made using the Fourier analysis (see 2.1.3) and decide when to stop the simulation. (see 2.1.3). It is also the one that computes the *inter-plants critical distance* (IPCD) (see below).

Managing the Row Agents. At the beginning of the simulation, the DA analyses the rows detected using the Fourier analysis in an attempt to exclude the false positives: rows that are only made out of weeds. A special procedure is devised to do so based on the fact that these will be positioned in between real RAs (rows consisting in plants).

Computing the Inter-Plants Critical Distance (IPCD). Most of the decisions of the agents depend

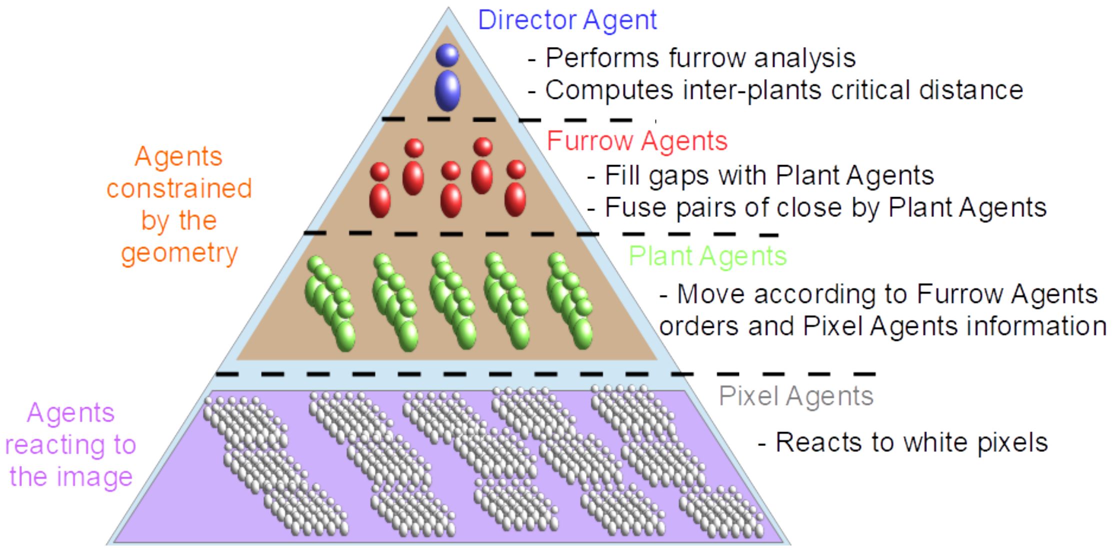

Figure 3: Hierarchical architecture of the multi-agent system.

on the IPCD. It is set equal to the maximum of the density distribution of the inter-plant distances.

2.2.2 The Pixel Agents

The PXAs sense the Otsu images and are instantiated by a PA. They become *activated* if they are positioned on a white pixel and their position is determined by the PA they are dependent upon.

2.2.3 The Plant Agents

The PAs are ultimately the most important agents for the plant counting task. The number of PAs at the end of the simulation determines the number of plants detected in the frame of the image. Each PA has under its supervision a group of PXAs that is centered on the position of the PA. The role of the group of PXAs is to guide the PA toward the most white parts of an Otsu image (i.e. guiding them toward plants). Therefore, at step $i+1$ of the simulation, a PA moves on the mean point of all its activated PXAs at step i:

$$(PA_x^{i+1}, PA_y^{i+1}) = \left(\frac{1}{n}\sum_{PXA\in\mathcal{A}} PXA_x^i, \frac{1}{n}\sum_{PXA\in\mathcal{A}} PXA_y^i\right) \quad (1)$$

with $\mathcal{A}$ the set of activated PXAs. The x and y are the positions of the agents. Finally, a PA can decide to decrease or increase its sensing area by eliminating PXAs or by initializing new PXAs. In our simulations, we set the goal of the PA to have between 20% and 80% of its PXAs activated.

2.2.4 The Row Agents

RAs are instantiated by the DA according to the rows detected by the Fourier Analysis (Fig. 2, item **2**). In turn, each RA first initializes as many PAs as were detected using the Fourier analysis (Fig. 2, item **4**). Because the Fourier analysis may miss plants at the edges of the rows detected, additional PAs are evenly spaced at 1.1ν times the IPCD, ν being the PAs fusing factor (see next paragraph). At each simulation's step, RAs eliminate the PAs that are located in black areas of the Otsu image: PAs with less than a proportion δ of activated PXAs .

Filling and Fusing PAs. A RA may consider that the distance between two consecutive PAs is either too large or too small. It then decides to either fill in the gaps with new PAs of fuse the two involved PAs:

$$Decision = \begin{cases} \text{Fill} & if\ |PA_y^{i+1} - PA_y^i| > \mu\, IPCD \\ \text{Fuse} & if\ |PA_y^{i+1} - PA_y^i| < \nu\, IPCD \end{cases} \quad (2)$$

with μ and ν the filling and fusing factor respectively.

Constraining PAs Movements. In a crop field, the rows usually exhibit a linear shape, aligned with the Y axis when adjusting the images (Section 2.1.2). The plants that are part of the same row are thus expected to be aligned. As a consequence, a RA can constrain the moves of the PAs that it supervises in order to keep them as aligned as possible.

2.2.5 Running the Simulation

The simulation consists in a sequence of actions that the agents carry out in a deterministic order (Algo. 1). The final count of the plants occurs when the number of PAs remains constant.

Algorithm 1: Simulation.

```
Input: max_nb_steps, μ, ν, δ, π
initialize DA, RAs, PAs, PXAs
/* Sec. 2.2.1 */
AnalyseRows(π)
ComputeIPCD()
AnalyseRowsEdges(ν, IPCD)
StopSimu ⟵ False
RE_Eval ⟵ False
i ⟵ 1
while i ≤ max_nb_steps & StopSimu = False do
    /* Sec. 2.2.3 */
    MoveToMeanPoint()
    /* Sec. 2.2.4 */
    ConstrainPAsXMovement()
    FillOrFusePAs(μ, ν, IPCD)
    /* Sec. 2.2.3 */
    AdaptSize()
    /* Sec. 2.2.4 */
    DestroyLowActivityPAs(δ)
    if Nb_PAs_i − Nb_PAs_{i−1} = 0 then
        if RE_Eval = False then
            DA_ComputeIPCD()
            RE_Eval ⟵ True
        else
            StopSimu ⟵ True
        end
    else
        RE_Eval ⟵ False
    end
    i⟵ i+1
end
```

3 SYNTHETIC DATASETS

Training an automatic counting algorithms requires large data sets with at the very least hundreds of images, with thousands of objects, each of them to be labeled. In the case of plant counting, there are no publicly available data sets. This entails a lack of labeled training data and a problem of reproducibility

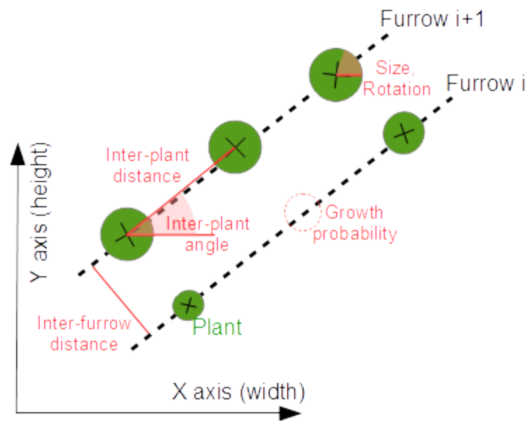

Figure 4: Parameters involved in the placement of crops along rows. The red labels are parameters undergoing randomization.

of experiments.

The solution we adopted is to use a virtual environment engine to generate artificial crop fields. They are indeed nowadays able to generate very realistic images, and the labelling of the objects is automatic. We chose to use the game engine Unity (Technologies, 2020).

3.1 The Field Generator

The parameters mainly manage the surface of the field, the virtual crop, the weed, the sun and the simulated drone. Figure 5 describes the UAV flight plan. Crops position in the field are based on several parameters shown in red on Figure 4. All parameters except the *growth probability* are drawn randomly. Weeds cannot be expected to follow any geometry at the scale of the field but they can regularly be found clustered together. This is why we used the Perlin Noise (Perlin, 1985) to generate spaces on the crop field where the weeds would be present.

3.2 Content of the Datasets

Plants may overlap as the plants grow. It is assumed that the overlap interferes with the signal used by the counting method, and previous studies on automatic counting of plants from UAV images have raised that the difficulty of the task increases with the proportion of crop overlap (García-Martínez et al., 2020). In order to assess this effect, we generated three datasets with three different levels of overlap between crops.

The plants are separated (S) from each other in the first dataset; they overlap for some leaves and do not overlap for others (B) in the second datase; and finally, the third dataset exhibits overlap (O) between neighbouring plants. The dataset (S) is considered

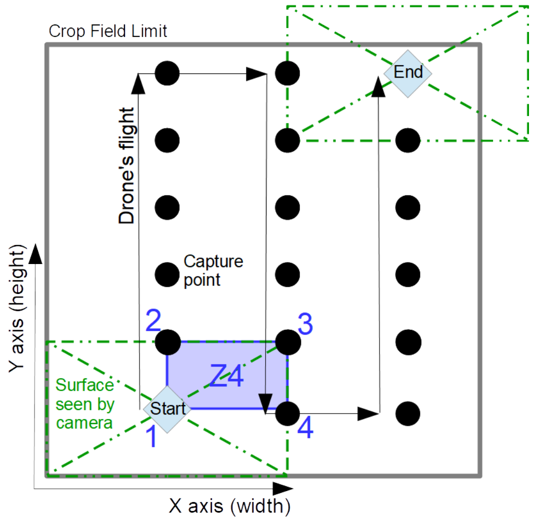

Figure 5: Scheme of a UAV flight plan above the virtual crop field. The start position is calibrated to capture the bottom left corner of the field. The other capture points are calculated depending on the image overlap configured on the X and Y axis (here, 50% on both). As a result, the images of the upper and right limit of the field may go over these. The area named *Z4* is subsequently captured four times, one by each of the four captured points numbered in blue.

easy, (B) is intermediate and (O) is difficult. Aside from varying the scale of the plant 3D model to simulate its growth, the parameters used to generate the fields are similar for all three datasets. Each crop field was generated with an inter-rows distance of 70 *cm* and an inter-plants distance of 20 *cm* with 5% variability. This yields a target average of 7 $plants/m^2$ which matches typical sunflower crop fields. The plant growth probability was set to 0.8. The Perlin noise threshold used to generate the surfaces where weed grows was set to 0.75 while the weed growth probability was set to 0.6. In each of these datasets, 100 crop fields were generated, and from each of them four images were taken. So, each dataset contains 400 images which amounts to 1200 images in total. To take pictures of the virtual fields, we simulated a short drone flight plan that covers the lower left corner of the field as it moves once along the height and width of the field (see the blue numbers on Fig. 5). We have configured the motion of the simulated drone to overlap the image by 50% along both their height and width, as is usual with images from UAVs.

Fig. 6 gives an example of an image of a virtual crop field. Fig. 6b is the same image after an Otsu filter has been applied and the image has been reoriented so that the rows are aligned with the Y axis. (see sections 2.1.1 and 2.1.2).

4 EXPERIMENTS AND RESULTS

The method we propose is a two steps method with the first phase that detects and estimates the spatial structure, and the second phase which, starting from this structure identifies the objects.

The goal of the experiments carried out is threefold. *First*, to assess the performance of the first phase alone in counting plants, *second*, to measure the added value of the second phase based on a multi-agent approach, and, *third*, to look at the gain of performance, if any, when parts of a field are covered by multiple passes of the UAV and a redundancy of information follows (see area *Z4* in Figure 5 for an example).

First, we present the rules under which we considered that the method had successfully detected a plant and how the counting performance was measured.

4.1 Assessing the Results

In order to measure the performance of the Fourier analysis alone, the rule is that if the plant position, which is known in synthetic data sets, falls within a 40 square pixel area of a predicted position, then this is counted as a true positive (TP).

For the MAS, we considered that a PA detected a plant if that plant was located within the sensing area defined by the PXAs of the PA. If two PA happen to detect the same plant, then only one PA is counted as TP and the other is counted as a false positive (FP). Additionally, a PA or a prediction from the Fourier analysis that does not contain a plant in their sensing area are also considered as FP. Finally, a plant that has not been detected is counted as a false negative (FN). In addition to these three indicators, three scores are computed:

$$\text{Detection Accuracy} = \frac{TP}{\text{Total number of PAs}} \quad (3)$$

$$\text{Detection Recall} = \frac{TP}{\text{Total number of Plants}} \quad (4)$$

$$\text{Counting Accuracy} = \frac{\text{Total number of PAs}}{\text{Total number of Plants}} \quad (5)$$

These scores are later referenced as *DAc*, *DR* and *CA* respectively.

In the following, we compare the performances of the Fourier analysis alone (Section 4.2), of the multi-agent approach from a single image of the area (Section 4.3), and of a technique that takes into account that several images (up to four) can cover a given area (Section 4.4).

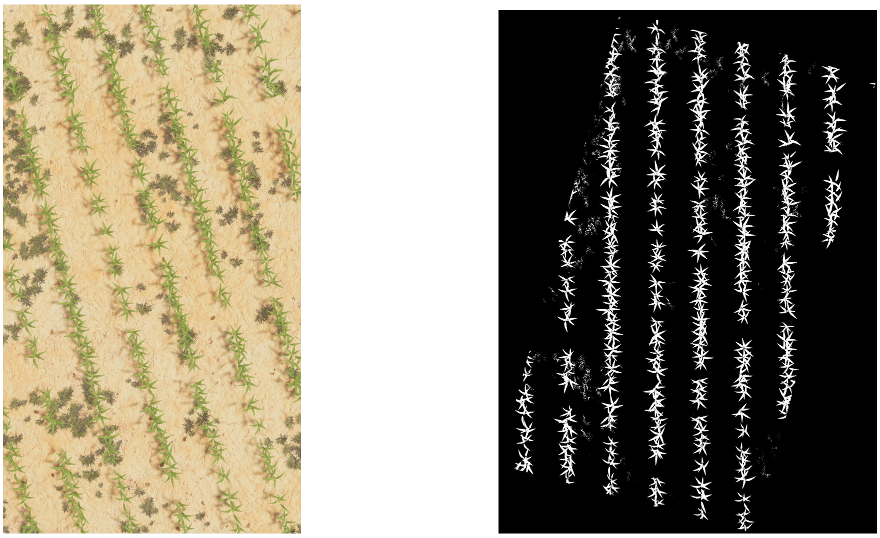

(a) An image of a virtual field (b) Otsu image vertically adjusted

Figure 6: Example of a an synthetic image and its vertically adjusted Otsu image.

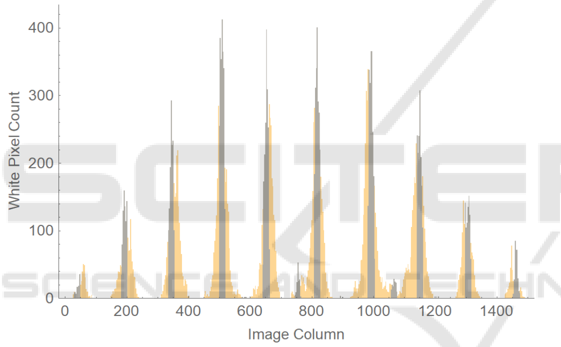

Figure 7: Example of row detection thanks to Fourier analysis. The histogram in yellow results from the projection of the white pixels of an Otsu Image on the X axis. The blue parts of the histogram are the detected rows.

4.2 Detecting the Spatial Structure and Counting

As explained in Section 2.1.3, we use Fourier analysis to approximate the spatial structure in an image. We first try to discover the rows and then to locate plants within the presumed rows. This relies on the analysis of the density distribution of the projection of the white pixels from an Otsu image on the X or Y axis (Fig. 7 shows such a density distribution (in yellow) as well as the detected peaks (in blue)). Notice that the largest peaks indeed correspond to rows, but that weeds can also produce peaks, albeit smaller ones.

The results obtained for the three scores are summarized in Table 1 in the line *Fourier* while Fig. 8 provides details on the distribution of the counting accuracies (CAs) (violet boxes indicate the results of the Fourier analysis).

It is apparent that the Fourier analysis alone tends to underestimate the number of plants on dataset (S), (the well separated plants) (12% on average) while over estimating this number on datasets (B) (between separated and overlapping) (by 3%) and (O) (overlapping plants) (by 7% on average). Why is it so?

For dataset (S), the plants are well separated, but this also entails that the peaks of the histogram used by the Fourier analysis are rather narrow, and one consequence is that if a peak is slightly off a predicted position by the analysis, it may be entirely missed by it. This may result in ignoring existing rows or plants within a row.

For datasets (B) and (O), the overlapping leaves between plants induces noise that leads the Fourier analysis dedicated to the plants identification to find a slightly higher frequency than the actual target. This results in overestimating the number of plants. Overall, still, taking into account that the Fourier analysis is in fact used only to estimate the spatial relationships between plants on crop fields, the counting results are surprisingly good.

4.3 Effect of the Multi-Agents Analysis

The multi-agent stage initializes the PAs using the predictions made by the detector of spatial relationships, and then let the PAs evolve and converge towards presumed plants. The question is: how much this can improve the counting performance? In which way can it correct false positives and false negatives?

In our experiments on plant counting, we ran

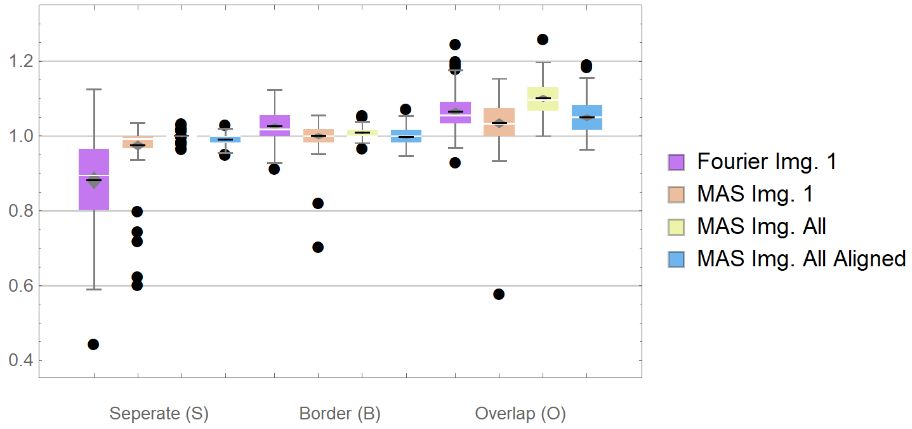

Figure 8: Results on Counting Accuracy (CA). The colors of the whisker boxes indicate the method used to count the number of plants. With *Fourier Img. 1* we counted the plants with the Fourier analysis on one imagefor each of the 100 fields of the dataset. The same images were used with *MAS Img. 1* that counts the plants using the MAS. *MAS Img. All* and *MAS Img. All Aligned* are methods that exploit the redundancy when several images cover the same area in a field. The black dots represent outliers. The boxes' lower and upper limits indicate the 0.25-th and 0.75-th percentile respectively. The median is represented on each box by a white line mark while the mean is represented as a black line mark. The grey diamond represents the interval of confidence. Non-overlapping diamond between pairs of boxes are equivalent to rejecting the null hypothesis of equal means of a two-sample t-Test.

the simulations with the following parameters values: max_nb_steps $= 50$, $\mu = 1.5$, $\nu = 0.5$, $\delta = 0.01$ and $\pi = 0.0001$. *max_nb_steps* was set as an upper limit of the number of steps of the simulation which has never been reached in our experiments. The values μ and ν were chosen for geometric reasons. ν is the PAs' fusion factor; a value of 0.5 means that two PAs perfectly positioned on consecutive plants will absorb a wrongly positioned PA in-between them which is desirable. μ is the PAs' filling factor; if two PAs are perfectly positioned on plants but another plant has been missed in-between them, then a value of 2 should allow its detection. However a value of 1.5 proved to be better during tests. Lowering the values of δ and π will lead the simulation to overestimate the number of plants while raising them will lead to underestimation. These values were optimized by repeatedly testing the system on training synthetic datasets. The reported results have been obtained on test datasets, different from the training ones.

As can be seen in Fig. 8 and in Table 1, the results show that the multi-agent phase significantly improves the counting performance. For the (S) and (B) datasets, the mean value is closer to the value 1 (approximately 0.98 instead of 0.87 for the Fourrier analysis alone), which means that the estimated number of plants is close to the correct one, and the confidence interval is much narrowed (standard deviation of 0.04 instead of 0.11). The gain is less pronounced on the (O) dataset. Even if the distribution of the results are very similar between the Fourier analysis and the multi-agent one (violet and orange boxes on Fig. 8), the average for the multi-agent analysis is significantly lower than the average of the Fourier analysis as indicated by the fact that the grey diamonds on the boxes do not overlap (non-overlapping diamonds mean that the null hypothesis of equal means can be rejected using a 2-sample t-Test).

It is thus apparent that the proposed two step method: first detecting a structure, then using a MAS to refine the counting, gives very promising results. But, most of the areas of a crop field are covered by several different images from UAVs (up to four times in the example of Figure 5). Is it possible then that even these good results can be improved by resorting to the redundancy thus offered?

4.4 Exploiting Image Overlapping

A common practice when acquiring images of crop fields is to let consecutive images overlap each other. One of the main motivation for this is to avoid that plants located at the edges of an image are only partially visible, and thus ignored. Another motivation is the hope that the mistakes made on an image can be compensated on another image that partially covers the same area. In our case, the synthetic datasets were built with 50% overlap on the height and width of the images. As an illustration, in our example, it exists an area (e.g. *Z4*) that is covered by all four images. The results when combining the informations coming from the four images are presented under the name *MAS Img. All* in Table 1 and Fig. 8. Another variant of this algorithm (called *MAS Img. All Aligned*)

Table 1: Average scores results on the three datasets. Standard deviation is in parenthesis. Values were rounded to the second digit.

Datasets	Separate (S)			Border (B)			Overlap (O)		
Scores	DAc	DR	CA	DAc	DR	CA	DAc	DR	CA
Fourier Img. 1	0.93 (0.04)	0.82 (0.11)	0.88 (0.12)	0.87 (0.06)	0.89 (0.05)	1.03 (0.04)	0.81 (0.05)	0.86 (0.05)	1.07 (0.05)
MAS Img. 1	0.99 (0.01)	0.97 (0.07)	0.97 (0.07)	0.98 (0.02)	0.98 (0.04)	**1.00** (0.04)	0.83 (0.05)	0.86 (0.06)	**1.03** (0.07)
MAS Img. All	0.99 (0.01)	0.99 (0.01)	**1.00** (0.01)	0.99 (0.02)	1.00 (0.01)	1.01 (0.02)	0.88 (0.04)	0.96 (0.02)	1.10 (0.05)
MAS Img. All Aligned	0.99 (0.01)	0.98 (0.01)	0.99 (0.02)	0.99 (0.02)	0.98 (0.02)	**1.00** (0.02)	0.90 (0.04)	0.94 (0.03)	1.05 (0.05)

was introduced with the motivation that aligning the N images covering a given area could help the clustering procedure to gather relevant PAs.

The results reported in Table 1 and in Figure 8 show that combining information from the analysis of several images brings improvement in the counting accuracy for the (S) and (B) datasets. For the (O) dataset, the variant *MAS Img. All Aligned* is to be preferred to the *MAS Img. All* method, while *MAS Img. All* is better than *MAS Img. All Aligned* on the (S) and (B) datasets. If the counting accuracy of the combined method is slightly lower than for the method analyzing only one image for the (O) datasets (1.05 instead of 1.03), on the other hand the detection accuracy (DA) is significantly improved from 0.83 to 0.90 which means that the plants are better recognized.

Overall, combining information from several images seems to be a good strategy.

4.5 Application to Real Images

We also applied the method to a subset of the dataset of real crop fields provided by Christophe Sausse from *Terres Inovia*.

In total, the dataset contains 2111 non-labelled images from which we randomly extracted 50 that were manually labeled and used to test our method. The images mix areas where the plants are well separated and areas where the leaves of one plant overlap with those of its neighbors in the same row. In addition, the drone captured the original images at an altitude of 30m (compared to 10m for the synthetic data) and the sunflowers overlap with many weeds in some images, making it sometimes difficult, even for a human, to visually identify the sunflowers. It is thus fair to say that the chosen subset of data contains images comparable to the ones of the (S), (B) and (O) synthetic datasets.

Our method yielded an average counting accuracy of 1.03 for a standard deviation of 0.12 on the 50 images subset. The detection accuracy and detection recall fared at 0.87 and 0.90 respectively for a standard deviation of 0.14 for both. These scores are at least as good as the ones reported in the state of the art (see Section 4.6). Furthermore, they are quite close to the results obtained on the synthetic dataset even if the standard deviation is larger.

This confirms that using synthetic datasets for tuning the method we propose is a promising procedure, effectively leading to good results on real data.

4.6 The State of the Art

Counting objects can be done through the detection of the objects, or it can be done from a density estimate, usually directly from an analysis at the pixel level of the image. In the first case, object detection relies either on some prior knowledge of the shape of the objects to be counted or on machine learning to recognize objects. Deciding which templates are useful is generally difficult, while using supervised learning requires (very) many labeled images and large computing resources, for example using deep neural networks. On the other hand, density estimation seems simpler but it still requires large training sets and yields coarser estimates of the number of objects in an image. Both approaches, object-based and density-based, are subject to large errors when objects are occluded or overlapping.

For plant counting, (García-Martínez et al., 2020) is an example of the template approach. In their maize plant counting experiments, they selected 4 to 12 templates and used a Normalized Cross-Correlation technique to estimate the number of plants. The method requires that representative plants in the images be chosen, and no recipe is given for this. They obtain a percentage or error of 2.2% when using 12 templates, but acknowledge that the performance drops to 25.7% when the plants overlap.

In their paper, (Ribera et al., 2017) use deep neural networks to learn how to recognize sorghum plants. They describe the rather involved preprocessing and formatting steps that are necessary before learning can take place. They also had to develop a technique to increase the number of labelled training images. Learning itself took between 50,000 and 500,000 iterations which entails a very heavy computing load. They obtained a Mean Absolute Percentage Error of 6,7%. It is not possible to know if the data sets used included overlapping plants or not.

The density-based approach is illustrated in (Gnädinger and Schmidhalter, 2017). They first eliminate what can be presumed to be weeds and parasitic signals using a clustering method. Then they set thresholds on different wavelengths in order to classify pixels as belonging to plants or not. This requires some fine tuning. They obtain error rates around 5% with fairly large standard deviations. Here too, plant overlapping leads to a deterioration in performance.

5 CONCLUSIONS

With the generalization of devices for taking images, it is increasingly critical to develop reliable and transparent image vision systems (Olszewska, 2019). This paper has introduced a new method to count objects while satisfying these constraints. It is applicable when objects are spatially organized according to a regular pattern. The method first detects the pattern and then uses it to seed agents in a MAS. The method is simple, requiring no complex fine tuning of parameters, the tricky definition of templates or costly learning. In fact, it requires very modest computing resources. In a series of extensive experiments on controlled data sets and real aerial images of crop fields, the method yielded state of the art or better performance when the objects are well-separated and exceeded the best known performances when the objects overlap. For future work, we plan to test the method on other other object counting problems with different geometries such as counting people in stadiums or performance halls or vehicles in parking lots.

ACKNOWLEDGEMENTS

We thank *Terres Inovia* for sharing their dataset of crop fields images captured with a UAV.

REFERENCES

García-Martínez, H., Flores-Magdaleno, H., Khalil-Gardezi, A., Ascencio-Hernández, R., Tijerina-Chávez, L., Vázquez-Peña, M. A., and Mancilla-Villa, O. R. (2020). Digital count of corn plants using images taken by unmanned aerial vehicles and cross correlation of templates. Agronomy, 10(4):469.

Gnädinger, F. and Schmidhalter, U. (2017). Digital counts of maize plants by unmanned aerial vehicles (uavs). Remote sensing, 9(6):544.

Guerrero, J. M., Pajares, G., Montalvo, M., Romeo, J., and Guijarro, M. (2012). Support vector machines for crop/weeds identification in maize fields. Expert Systems with Applications, 39(12):11149–11155.

Guijarro, M., Pajares, G., Riomoros, I., Herrera, P., Burgos-Artizzu, X., and Ribeiro, A. (2011). Automatic segmentation of relevant textures in agricultural images. Computers and Electronics in Agriculture, 75(1):75–83.

Han, S., Zhang, Q., Ni, B., and Reid, J. (2004). A guidance directrix approach to vision-based vehicle guidance systems. Computers and Electronics in Agriculture, 43(3):179–195.

Hofmann., P. (2019). Multi-agent systems in remote sensing image analysis. In Proceedings of the 11th International Conference on Agents and Artificial Intelligence - Volume 1: ICAART 2019, pages 178–185. INSTICC, SciTePress.

Olszewska, J. (2019). Designing transparent and autonomous intelligent vision systems. In Proceedings of the 11th International Conference on Agents and Artificial Intelligence - Volume 2: ICAART 2019, pages 850–856. INSTICC, SciTePress.

Otsu, N. (1979). A Threshold Selection Method from Gray-Level Histograms. IEEE Transactions on Systems, Man, and Cybernetics, 9(1):62–66. Conference Name: IEEE Transactions on Systems, Man, and Cybernetics.

Pérez-Ortiz, M., Peña, J. M., Gutiérrez, P. A., Torres-Sánchez, J., Hervás-Martínez, C., and López-Granados, F. (2016). Selecting patterns and features for between-and within-crop-row weed mapping using uav-imagery. Expert Systems with Applications, 47:85–94.

Perlin, K. (1985). An image synthesizer. ACM SIGGRAPH Computer Graphics, 19(3):287–296.

Ribera, J., Chen, Y., Boomsma, C., and Delp, E. J. (2017). Counting plants using deep learning. In 2017 IEEE global conference on signal and information processing (GlobalSIP), pages 1344–1348. IEEE.

Technologies, U. (2020). Unity 2019.4.1.

Zou, Z., Shi, Z., Guo, Y., and Ye, J. (2019). Object Detection in 20 Years: A Survey. arXiv:1905.05055 [cs]. arXiv: 1905.05055.